

Optimizing thermal transport in the Falicov-Kimball model: binary-alloy picture

J. K. Freericks¹ and V. Zlatić²

¹*Department of Physics, Georgetown University, Washington, DC 20057-0995, U.S.A.*

²*Institute of Physics, Zagreb, Croatia*

(November 16, 2018)

We analyze the thermal transport properties of the Falicov-Kimball model concentrating on locating regions of parameter space where the thermoelectric figure-of-merit ZT is large. We focus on high temperature for power generation applications and low temperature for cooling applications. We constrain the static particles (ions) to have a fixed concentration, and vary the conduction electron concentration as in the binary-alloy picture of the Falicov-Kimball model. We find a large region of parameter space with $ZT > 1$ at high temperature and we find a small region of parameter space with $ZT > 1$ at low temperature for correlated systems, but we believe inclusion of the lattice thermal conductivity will greatly reduce the low-temperature figure-of-merit.

Primary: 72.15.Jf; 72.20.Pa, 71.20.+h, 71.10.Fd

I. INTRODUCTION

There has been a recent resurgence of interest in solid-state devices for thermoelectric applications¹ (power generation or cooling). The recent focus has been on investigating strongly correlated materials, which may prove to have better performance than the current generation of semiconductor-based devices. The two main areas of application for thermoelectrics are in power generation from the Peltier effect,² where heat energy is converted into electricity; and in thermoelectric cooling, where an electrical current is driven through a device to force heat to move from the cold to hot end. Power generation applications typically operate at temperatures higher than 1000 K, with the heat source being a radioactive material (for applications in the space industry) or a combustion source. Thermoelectric coolers usually operate around room temperature, and the semiconductor-based devices do not function below about 200 K. Currently, thermoelectric devices fit niche markets, where reliability, size, or weight are more important than efficiency. The coolers usually operate with relatively low heat loads because of their poor efficiency.

The efficiency of a thermoelectric device is a function of the dimensionless product of a materials parameter denoted Z with the average temperature T (between the hot and cold heat sources of the device) and is called ZT . It satisfies

$$ZT = \frac{T\sigma_{dc}S^2}{\kappa_e + \kappa_l}, \quad (1)$$

and the term $\sigma_{dc}S^2$ in the numerator is often called the power factor. Here we have σ_{dc} the dc electrical conductivity, S is the Seebeck coefficient,³ T is the temperature, κ_e is the electronic contribution to the thermal conductivity, and κ_l is the lattice contribution to the thermal conductivity (we are assuming the electron-phonon interaction is small enough that these two effects can be decoupled). It is commonly stated that $ZT > 1$ is needed for operation of thermoelectric devices, but this is not

necessarily true.⁴ For example, if we consider a thermoelectric cooler operating at 300 K and with 50 K of cooling, then one can operate such a device for $ZT > 0.7$, but one would need $ZT \approx 4$ to achieve the coefficient of performance of a conventional compressor-based refrigerator (which lies in the 1.2 – 1.4 range). Nevertheless, most commercial thermoelectric devices have ZT near 1 because no materials have been discovered with much larger values. Of course there is significant interest in increasing ZT by a factor of 4 at room temperature (to be competitive with conventional coolant-based technology), or to above 1 at low temperature to allow for new applications such as solid-state coolers for superconducting electronics or infrared detectors.

Although there are no fundamental thermodynamic limitations⁵ to the size of ZT , it has proved to be quite difficult to find materials with $ZT > 1$ over a wide temperature range, and to find much larger values of ZT (say $ZT > 3$). Recently, Rontani and Sham⁶ proposed that heterostructures of correlated semiconductors and metals could have dramatically large values of ZT at low temperature. Their idea was that if one tuned the large electronic density of states (DOS) of the f -electrons to lie close to the fermi level, then one could produce huge values of ZT (earlier work proposed similar ideas as well⁷). Mahan and Sofo⁸ also argued in the same vein for optimization in bulk materials in 1996. But so far, no one has been able to demonstrate that such large values of ZT are possible in a true many-body system (and are not the artifact of some approximations employed in the analysis). We examine this problem in detail for the Falicov-Kimball model here. By working in the limit where the ion concentration is fixed and nonzero at $T = 0$, we have adjusted the renormalized energy level of the ion to lie at the electronic chemical potential, which has the potential for producing large thermoelectric responses.

Mahan and Sofo⁸ also proved that the figure-of-merit always satisfies an inequality

$$ZT < \frac{\kappa_e + T\sigma_{dc}S^2}{\kappa_l} \quad (2)$$

regardless of the strength of the many-body interactions. This has important implications for theorists, because in purely electronic models, such as the one we investigate here, $\kappa_l = 0$, so there is no *a priori* limitation on the magnitude of ZT . But it also presents some problems for low- T calculations, since the electronic contribution to the thermal conductivity is usually much smaller than the lattice contribution at low temperature (especially for insulators), and hence *purely electronic estimates of ZT can be greatly enhanced when the lattice effects are ignored*. This becomes less of an issue at high temperature, where the electronic contribution to the thermal conductivity can dominate.

Another interesting feature that plagues the low- T regime is the fact that in most systems $S \rightarrow 0$ as $T \rightarrow 0$. Since the ratio of the conductivities often satisfies the Wiedemann-Franz law

$$\frac{\kappa_e}{\sigma_{dc}} = \left(\frac{k_B}{e}\right)^2 \mathcal{L}T \quad (3)$$

with \mathcal{L} the Lorenz number (equal to $\pi^2/3$ in a fermi liquid and 3 in an intrinsic semiconductor), we have $ZT \rightarrow 0$ if $S \rightarrow 0$ at low temperature. Similarly, if $S(T)$ suffers a sign change at any T , then ZT will be quite low in the vicinity of the sign change.

The Falicov-Kimball model⁹ appears to be able to describe an increasing number of materials and systems. One example, that fits within the binary-alloy picture, is tantalum deficient tantalum nitride¹⁰ Ta_xN . This material is metallic when $x = 1$ but becomes a fairly large-gap insulator (about 1.5 eV) when $x = 0.6$. If we let the A ion denote a unit cell with a Ta atom, and a B ion denote a unit cell with no Ta atom, then U is the difference in site energies for the two configurations. The total conduction electron concentration also depends on the Ta vacancies, as each vacancy can bind 5 electrons. It is easy to model the metal-insulator transition at $x = 0.6$ by properly varying the electron concentration with the concentration of Ta vacancies.

In Section II we develop the formalism for deriving the dc conductivity, the thermopower and the thermal conductivity. We use this to determine both the Lorenz number and the figure-of-merit. In Section III we provide numerical results for the thermal transport illustrating regimes where ZT can become large, and describing the physical principles that drive such enhancements. In addition, we describe in detail the situation behind a large figure-of-merit at low- T and whether achieving such a goal is feasible. Conclusions are presented in Section IV.

II. FORMALISM FOR THE THERMAL TRANSPORT

The Hamiltonian we study is the spinless Falicov-Kimball model⁹ with a canonical-binary-alloy picture

$$H = -\frac{t^*}{2\sqrt{d}} \sum_{\langle i,j \rangle} c_i^\dagger c_j + U \sum_i w_i c_i^\dagger c_i, \quad (4)$$

where c_i^\dagger (c_i) is the electron creation (annihilation) operator for a spinless electron at site i (spin can be included trivially if desired by doubling all of the L_{ij} defined below), w_i is a variable that equals zero or one and corresponds to the presence of an A ion ($w_i = 1$) or the presence of a B ion ($w_i = 0$) at site- i , and U is the interaction strength (difference in the site energy between the A and B ions). The hopping integral is scaled with the spatial dimension d so as to have a finite result in the limit¹¹ $d \rightarrow \infty$; we measure all energies in units of $t^* = 1$. We work on a hypercubic lattice where the noninteracting density of states is a Gaussian $\rho(\epsilon) = \exp(-\epsilon^2)/\sqrt{\pi}t^*\Omega_{uc}$ (with Ω_{uc} the volume of the unit cell). A chemical potential μ is employed to adjust the conduction electron filling ρ_e .

The Falicov-Kimball model can be solved exactly by employing dynamical mean field theory^{12,13}. A review that describes how to solve for the Green's function using the equation of motion technique has recently appeared.¹⁴ Because the self energy $\Sigma(z)$ has no momentum dependence, the local Green's function satisfies

$$G(z) = \int d\epsilon \rho(\epsilon) \frac{1}{z + \mu - \Sigma(z) - \epsilon}, \quad (5)$$

with z a complex variable in the complex plane. The self energy, local Green's function, and effective medium G_0 are related to each other by

$$G_0^{-1}(z) - G^{-1}(z) = \Sigma(z), \quad (6)$$

and the Green's function also satisfies

$$G(z) = (1 - w_1)G_0(z) + w_1 \frac{1}{G_0^{-1}(z) - U}. \quad (7)$$

Here w_1 is the average concentration of the A ions (which is an input parameter). The algorithm for determining the Green's function begins with the self energy set equal to zero. Then Eq. (5) is used to find the local Green's function. The effective medium is found from Eq. (6). The new local Green's function is then found from Eq. (7) and the new self energy from Eq. (6). This algorithm is repeated until it converges.

When these equations are solved we find a number of interesting results for the single-particle properties. First, both the interacting DOS [$\rho_{int}(\omega) = -\text{Im}\{G(\omega + i\delta)\}/\pi$] and the self energy on the real axis are independent of temperature¹⁵ when w_1 and μ are fixed (all of the temperature dependence for fixed ρ_e arises from the temperature dependence of μ , which shifts the zero-frequency point of the DOS). Second, we find that the self energy does not display fermi-liquid properties unless $U = 0$, $w_1 = 0$ or $w_1 = 1$ (which are all noninteracting cases). In particular, we do find (for small enough U) that the imaginary part of the self energy is quadratic in ω , but

the curvature has the wrong sign, and the zero frequency value of the imaginary part of the self energy does not go to zero as $T \rightarrow 0$ (in fact, it remains fixed for all T). Third, the real part of the self energy is linear (for small enough U), but the slope has the opposite sign of what is seen in a fermi liquid. Finally, we see that if U is large enough, the DOS develops a gap, and if the electronic chemical potential lies in the gap, then the self energy has quite anomalous behavior (including developing a pole).

Transport properties are calculated within a Kubo-Greenwood formalism¹⁶. This relates the transport coefficients to correlation functions of the corresponding transport current operators (these are equal to the bare bubbles because there are no vertex corrections in the large-dimensional limit¹⁷). We need two current operators here—the particle current¹⁸

$$\mathbf{j} = \sum_q \mathbf{v}_q c_q^\dagger c_q, \quad (8)$$

(where the velocity operator is $\mathbf{v}_q = \nabla_q \epsilon(q)$, the band-structure is $\epsilon(q)$, and the Fourier transform of the creation operator is $c_q^\dagger = \sum_j \exp[iq \cdot \mathbf{R}_j] c_j^\dagger / N$ and the heat current^{19,18}

$$\begin{aligned} \mathbf{j}_Q &= \sum_q [\epsilon(q) - \mu] \mathbf{v}_q c_q^\dagger c_q \\ &+ \frac{U}{2} \sum_{qq'} W(q - q') [\mathbf{v}_q + \mathbf{v}_{q'}] c_q^\dagger c_{q'}, \end{aligned} \quad (9)$$

[where $W(q) = \sum_j \exp(-iq \cdot \mathbf{R}_j) w_j / N$].

The dc conductivity, thermopower and electronic thermal conductivity can all be determined from relevant correlation functions of the current operators. We define three transport coefficients L_{11} , $L_{12} = L_{21}$, and L_{22} . Then

$$\sigma_{dc} = e^2 L_{11}, \quad (10)$$

$$S = \frac{k_B}{|e|T} \frac{L_{12}}{L_{11}}, \quad (11)$$

and

$$\kappa_e = \frac{k_B^2}{T} \left[L_{22} - \frac{L_{12} L_{21}}{L_{11}} \right]. \quad (12)$$

One finds that the electric and thermal conductivities are always positive, but the thermopower can have either sign—a positive thermopower corresponds to electron-like transport and a negative thermopower to hole-like transport (we use the sign convention of Ashcroft and Mermin²⁰). The transport coefficients are found from the analytic continuation of the relevant “polarization operators” at zero frequency

$$L_{11} = \lim_{\nu \rightarrow 0} \text{Re} \frac{i}{\nu} \bar{L}_{11}(\nu),$$

$$\bar{L}_{11}(i\nu_l) = \int_0^\beta d\tau e^{i\nu_l \tau} \langle T_\tau j_\alpha^\dagger(\tau) j_\beta(0) \rangle, \quad (13)$$

where $\nu_l = 2\pi T l$ is the Bosonic Matsubara frequency ($\beta = 1/T$), the τ -dependence of the operator is with respect to the full Hamiltonian in Eq. (4), and we must analytically continue $\bar{L}_{11}(i\nu_l)$ to the real axis $\bar{L}_{11}(\nu)$ before taking the limit $\nu \rightarrow 0$. Similar definitions hold for the other transport coefficients:

$$\begin{aligned} L_{12} &= \lim_{\nu \rightarrow 0} \text{Re} \frac{i}{\nu} \bar{L}_{12}(\nu), \\ \bar{L}_{12}(i\nu_l) &= \int_0^\beta d\tau e^{i\nu_l \tau} \langle T_\tau j_\alpha^\dagger(\tau) j_{Q\beta}(0) \rangle, \end{aligned} \quad (14)$$

and

$$\begin{aligned} L_{22} &= \lim_{\nu \rightarrow 0} \text{Re} \frac{i}{\nu} \bar{L}_{22}(\nu), \\ \bar{L}_{22}(i\nu_l) &= \int_0^\beta d\tau e^{i\nu_l \tau} \langle T_\tau j_{Q\alpha}^\dagger(\tau) j_{Q\beta}(0) \rangle. \end{aligned} \quad (15)$$

In all of these equations, the subscripts α and β denote the respective spatial index of the current vectors. Note that our definitions of the L_{ij} coefficients, while standard, have one less factor of T than seen in some other papers.

The analytic continuation is straightforward, and produces the Mott form²¹ for the transport coefficients (which is usually called the Jonson-Mahan theorem,¹⁹ and was explicitly evaluated for the Falicov-Kimball model²²):

$$L_{ij} = \frac{\sigma_0}{e^2} \int_{-\infty}^{\infty} d\omega \left(-\frac{df(\omega)}{d\omega} \right) \tau(\omega) \omega^{i+j-2}, \quad (16)$$

with the relaxation time $\tau(\omega)$ defined by

$$\tau(\omega) = \frac{\text{Im}G(\omega)}{\text{Im}\Sigma(\omega)} + 2 - 2\text{Re}\{[\omega + \mu - \Sigma(\omega)]G(\omega)\} \quad (17)$$

$f(\omega) = 1/[1 + \exp(\beta\omega)]$ and $\sigma_0 = e^2 \pi^2 / h d a^{d-2}$ on a hypercubic lattice in d -dimensions. Note that even though we represented the above form by an effective relaxation time, the above expression for the transport coefficients is *exact*.

Once the transport coefficients are known, we can determine the electrical and thermal conductivities and the thermopower. In addition, we find the figure-of-merit satisfies

$$ZT = \frac{L_{12}^2}{L_{11}L_{22} - L_{12}^2} \quad (18)$$

when we neglect κ_l and the Lorenz number becomes

$$\mathcal{L} \left(\frac{k_B}{e} \right)^2 = \frac{\kappa_e}{\sigma_{dc} T} = \left(\frac{k_B}{e} \right)^2 \frac{L_{11}L_{22} - L_{12}^2}{L_{11}^2 T^2}. \quad (19)$$

Note that because $-df(\omega)/d\omega$ is an even function of ω , only the even part of $\tau(\omega)$, $\tau_e(\omega) = [\tau(\omega) + \tau(-\omega)]/2$,

contributes to the L_{11} and L_{22} coefficients, and only the odd part $\tau_o(\omega) = [\tau(\omega) - \tau(-\omega)]/2$ contributes to L_{12} . Furthermore, one expects on general physical grounds that $\tau(\omega) \geq 0$. Indeed, this can be easily shown to be true by rearranging Eq. (17) into

$$\tau(\omega) = \int d\epsilon \rho(\epsilon) \frac{2[\text{Im}\Sigma(\omega)]^2}{\{[\omega + \mu - \text{Re}\Sigma(\omega) - \epsilon]^2 + [\text{Im}\Sigma(\omega)]^2\}^2} \quad (20)$$

which is manifestly nonnegative. In addition, we see that $\tau(\omega)$ vanishes whenever $\text{Im}\Sigma(\omega) = 0$. In the case of particle-hole symmetry, when $\rho_e = w_1 = 0.5$, it is easy to show that $\tau_o(\omega) = 0$, and both the thermopower and ZT must vanish.

We can employ the nonnegativity of $\tau(\omega)$ to show the Mahan-Sofa⁸ bound for ZT . The starting point is the fact that

$$\frac{\sigma_0}{e^2} \int_{-\infty}^{\infty} d\omega \left(-\frac{df(\omega)}{d\omega} \right) \tau(\omega)(\omega + a)^2 \geq 0 \quad (21)$$

which holds since all terms in the integrand are positive. Choosing $a = L_{12}/L_{11}$ then yields $L_{11}L_{22} - L_{12}^2 \geq 0$ (equality only occurs if the integrand is a delta function, which has no variance). Now the full expression for ZT can be written as

$$ZT = \frac{L_{12}^2/L_{11}L_{22}}{1 - L_{12}^2/(L_{11}L_{22}) + \kappa_l T/(k_B^2 L_{22})} = \frac{\xi}{1 - \xi + A} \quad (22)$$

by dividing the numerator and denominator in Eq. (1) by $k_B^2 L_{22}/T$. Here we used the notation $\xi = L_{12}^2/L_{11}L_{22}$ and $A = \kappa_l T/(k_B^2 L_{22})$. Using the fact that $\xi \leq 1$ then tells us that $\xi A \leq A \leq 1 - \xi + A$ since $1 - \xi \geq 0$. Dividing both sides of the inequality by $A(1 - \xi + A)$ then yields

$$ZT = \frac{\xi}{1 - \xi + A} \leq \frac{1}{A} = \frac{\kappa_e + T\sigma_{dc}S^2}{\kappa_l} \quad (23)$$

which is the Mahan-Sofa result. The inequality in Eq. (23) holds for any system that satisfies the Jonson-Mahan theorem, regardless of the many-body interactions present, as long as there is no electron-phonon coupling, which precludes the separation of the thermal conductivity into electronic and lattice pieces.

The integrals for the transport coefficients all have a derivative of the fermi function in them. This derivative becomes strongly peaked around $\omega = 0$ with a width on the order of T as $T \rightarrow 0$. In metals, we typically find that the relaxation time can be written in the form $\tau(\omega) = \tau_0 + w\tau' + O(\omega^2)$ for small ω . If we include only the first two terms in the expansion for the relaxation time, we find that

$$\begin{aligned} \sigma_{dc} &= \sigma_0 \tau_0 \\ S &= \frac{k_B \pi^2 \tau' T}{|e| 3} \end{aligned}$$

$$\kappa_e = \frac{k_B^2 \pi^2 \sigma_0 \tau_0 T}{e^2 3} \quad (24)$$

to lowest-order in T . We can read off that the Lorenz number \mathcal{L} is equal to $\pi^2/3$ and $ZT \rightarrow \pi^2 \tau'^2 T^2/3$ (when we neglect κ_l). Hence, ZT will be small in metals at low temperature because Wiedemann-Franz law fixes the ratio of conductivities, and the thermopower vanishes as $T \rightarrow 0$. If the Wiedemann-Franz rule holds at higher temperature as well, then one needs to find a thermopower larger than $\pi k_B/\sqrt{3}|e|$ which is equal to $156 \mu\text{V/K}$ in order to have $ZT > 1$ in a metal. There are no known metals that have thermopowers larger than $125 \mu\text{V/K}$ and most metals are one to two orders of magnitude smaller,⁵ so the only way to find metals that are useful for thermoelectric power generation or cooling is if the Wiedemann-Franz law does not hold.

The situation in an insulator is quite different. If we assume that $\tau(\omega) = \tau_0 \rho_{int}(\omega)$ with τ_0 a constant, and if we choose a generic interacting density of states that increases like a power law,

$$\begin{aligned} \rho_{int}(\omega) &= \theta(\omega - E_g/2)C(\omega - E_g/2)^\alpha \\ &+ \theta(-\omega - E_g/2)C'(-\omega - E_g/2)^{\alpha'} \end{aligned} \quad (25)$$

[with $\theta(x)$ the unit step function and E_g the insulating gap], then the behavior of the transport coefficients differs from Eq. (24). The starting point is to note that the number of holes excited in the lower band is equal to the number of electrons in the upper band, and at low temperature the fermi factors can be replaced by Boltzmann factors, resulting in

$$\int_{-\infty}^0 d\omega \rho_{int}(\omega) e^{\beta(\omega - \Delta\mu)} = \int_0^{\infty} d\omega \rho_{int}(\omega) e^{-\beta(\omega - \Delta\mu)} \quad (26)$$

with the chemical potential written as $\mu = \mu_0 + \Delta\mu(T)$. Solving for $\Delta\mu(T)$ yields

$$\begin{aligned} \Delta\mu(T) &\approx \frac{T}{2} \ln \left[\frac{\int_0^{\infty} d\omega \rho_{int}(\omega) \exp(\beta\omega)}{\int_{-\infty}^0 d\omega \rho_{int}(\omega) \exp(-\beta\omega)} \right] \\ &- \frac{T}{2} \ln \left[\frac{\int_0^{\infty} d\omega \rho_{int}(\omega) \exp(-\beta\omega)}{\int_{-\infty}^0 d\omega \rho_{int}(\omega) \exp(\beta\omega)} \right] \end{aligned} \quad (27)$$

with μ_0 the chemical potential at $T = 0$, which lies in the middle of the insulating gap (and is chosen to be the origin here). Using the form for the DOS in Eq. (25), then yields

$$\Delta\mu(T) = \frac{\alpha - \alpha'}{2} T \ln T + \frac{T}{2} \ln \left[\frac{C'\Gamma(\alpha' + 1)}{C\Gamma(\alpha + 1)} \right]. \quad (28)$$

This form for $\Delta\mu(T)$ plays an important role in the thermal transport of insulators. Indeed, an examination of the L_{11} and L_{12} coefficients in an insulator, with $T \ll E_g/2$, leads immediately to

$$L_{12} = L_{11} \left[\Delta\mu + \beta \frac{d\Delta\mu}{d\beta} \right], \quad (29)$$

which follows by taking the derivative of Eq. (26) with respect to β and using the definitions for L_{11} and L_{12} in the low-temperature limit. If $\Delta\mu(T) = 0$, as occurs at half filling, then we immediately see that $S = 0$ (as we also know must hold due to particle-hole symmetry). Furthermore, if $\Delta\mu(T)$ depends linearly on T , the thermopower vanishes linearly in T as well. S can approach a constant value if the low-temperature slope diverges [like in the $T \ln T$ dependence in Eq. (28)]. Divergent behavior can occur if $\Delta\mu(T)$ depends on T with a power-law less than 1 (and greater than 0), but it seems unlikely that one could find a circumstance where S will diverge like $1/T$ at low temperature (note that this argument does not hold for disordered insulators, that have localized states, so that the DOS does not vanish at the fermi level²³). Hence the qualitative temperature dependence of the thermopower in a correlated insulator can be determined by the temperature dependence of the chemical potential (at low T). Note that the above arguments obviously hold for intrinsic semiconductors as well.

If we use the generic insulator DOS in Eq. (25) and the approximation that $\tau(\omega) = \tau_0 \rho_{int}(\omega)$, then we find the following behavior for the transport in an insulator

$$\begin{aligned} \sigma_{dc} &= \frac{\sigma_0 \tau_0}{4} e^{-\beta E_g/2} \sqrt{\frac{C' T^{\alpha'} \Gamma(\alpha' + 1)}{C T^\alpha \Gamma(\alpha + 1)}} \\ S &= \frac{k_B}{|e|} (\alpha - \alpha') + \mathcal{O}(T) \\ \kappa_e &= \frac{\sigma_0 \tau_0}{4} e^{-\beta E_g/2} \sqrt{\frac{C' T^{\alpha'} \Gamma(\alpha' + 1)}{C T^\alpha \Gamma(\alpha + 1)}} \\ &\times \frac{k_B^2}{e^2} \left[\frac{E_g^2}{2T} - (\alpha' - \alpha)T \right]. \end{aligned} \quad (30)$$

The Lorenz number then diverges like $\mathcal{L} = E_g^2/2T^2$ at low temperature.

In a correlated insulator, we must have $\alpha = \alpha'$, so the thermopower vanishes linearly as $T \rightarrow 0$. This occurs because the interacting density of states develops a gap due to a pole in the self energy. Hence the band edge should have the same power law as that of the noninteracting system, which is determined by the van Hove singularity, and must be the same for the upper and lower band edge; the only place where this analysis might break down is at the critical coupling strength, where the gap initially opens, but we expect that the power-law dependence of the band edge may differ from the generic case, but it still should be equal for the upper and lower branches.

Unfortunately the hypercubic lattice in large dimensions does not behave like the generic insulator in the strong-coupling limit. This happens because the DOS never vanishes for a finite range of ω , but rather approaches zero exponentially for all nonzero ω (it is suppressed to zero precisely at $\omega = 0$ and $T = 0$). Hence we need to analyze the situation for the Gaussian DOS in more detail.

Inside the “gap region” of the DOS, the real part of

the self energy is large, because the self energy develops a pole at $\omega = 0$ in a correlated insulator. Similarly, the imaginary part of the self energy is very small. Hence, we can approximately determine the Hilbert transformation in Eq. (5) as

$$G(\omega) \approx \frac{1}{\omega + \mu - \text{Re}\Sigma(\omega)} - i\pi\rho[\omega + \mu - \text{Re}\Sigma(\omega)]. \quad (31)$$

Then we find from Eq. (6) that

$$G_0^{-1}(\omega) \approx \omega + \mu + i\{\text{Im}\Sigma(\omega) + \pi[\omega + \mu - \text{Re}\Sigma(\omega)]^2 \rho[\omega + \mu - \text{Re}\Sigma(\omega)]\}. \quad (32)$$

Next, by employing Eqs. (7) and (6), we finally determine that

$$\text{Re}\Sigma(\omega) \approx \frac{w_1 U (\omega + \mu)}{\omega + \mu - (1 - w_1)U} \quad (33)$$

and

$$\begin{aligned} \text{Im}\Sigma(\omega) &\approx -\pi \frac{(\omega + \mu)^2 (\omega + \mu - U)^2}{[\omega + \mu - (1 - w_1)U]^2} \rho \left[\frac{(\omega + \mu)(\omega + \mu - U)}{\omega + \mu - (1 - w_1)U} \right] \\ &\times \frac{w_1 (1 - w_1) U^2}{[\omega + \mu - (1 - w_1)U]^2 + w_1 (1 - w_1) U^2}. \end{aligned} \quad (34)$$

Now the local self energy of the correlated insulator has a pole at $\omega = 0$, hence we learn that $\mu_0 = (1 - w_1)U$ for the correlated insulator, and the interacting DOS is equal to zero at $\omega = 0$ (and $T = 0$). To lowest order, we find that the scattering time then satisfies

$$\tau(\omega) \approx \frac{[\omega + \mu - (1 - w_1)U]^4}{(\omega + \mu)^2 (\omega + \mu - U)^2 w_1 (1 - w_1) U^2} \quad (35)$$

which is a quartic dependence on frequency in the “gap region.” This implies that for the hypercubic lattice, the scattering time is much bigger than what one would guess from the approximation $\tau(\omega) = \tau_0 \rho_{int}(\omega)$ (which would be exponentially small).

We find that in our calculations, we usually have to input the imaginary part of the Green’s function and of the self energy by hand in the “gap region”, because the numerical precision of the computer does not allow them to be determined accurately with the iterative algorithm (the difficult step is constructing the self energy from the difference of the inverse of the local Green’s function and the effective medium, where numerical precision is lost). For accurate calculations, we need to go to higher order in our expansion than what was illustrated above, and since the real part of the self energy is determined reliably in the iterative algorithm, we construct the imaginary parts of the Green’s function and the self energy from the actual converged value of the real part of the self energy, rather than employing the asymptotic forms discussed above. Even with all of these tricks, it still is a challenge to determine a smooth $\tau(\omega)$ for the correlated insulator.

There is an advantage to studying the Falicov-Kimball model over the more popular Hubbard model,²⁴ because

the Falicov-Kimball model can be tuned to have a metal-insulator transition for any value of w_1 , simply by choosing U large enough and fixing $\rho_e = 1 - w_1$ [$\mu = (1 - w_1)U$]. The Hubbard model has a metal-insulator transition only at half filling, where the thermopower vanishes due to particle-hole symmetry (this can be broken by introducing multiband Hubbard models²⁵). Hence we can study effects of the correlated metal-insulator transition in the Falicov-Kimball model, that are inaccessible in the single-band Hubbard model. Since real materials typically have complicated bandstructures, one does not expect them to be particle-hole symmetric except in very special circumstances. Once again, the Falicov-Kimball model can be viewed as a more generic metal-insulator transition for making contact with real materials. The only disadvantage is that the Falicov-Kimball model is a non-fermi-liquid except in “noninteracting” limits (where it is a fermi gas).

III. NUMERICAL RESULTS

We present results at $\rho_e = 1 - w_1$ for three different values of U : (i) $U = 1$ which is a strongly correlated metal, that has a dip or kink in the interacting DOS at the fermi level; (ii) $U = 1.5$ which undergoes a metal-insulator transition as a function of w_1 ; and (iii) $U = 2$ which is a correlated insulator with a sizable “gap region”.

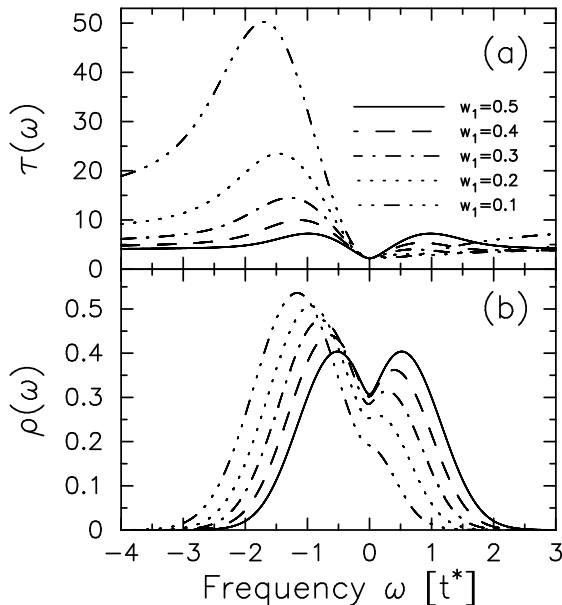


FIG. 1. (a) Effective scattering time and (b) interacting DOS for the Falicov-Kimball model at $U = 1$, $\rho_e = 1 - w_1$, and $w_1 = 0.5$ (solid), 0.4 (dashed), 0.3 (chain-dotted), 0.2 (dotted), and 0.1 (chain-triple-dotted). Note how both $\tau(\omega)$ and the DOS develop dips at the fermi level; both functions are symmetric at half filling $w_1 = 0.5$. These plots have fixed the origin at the $T \rightarrow 0$ limit of the chemical potential.

The effective scattering time and the interacting DOS are plotted in Fig. 1. We choose $U = 1$, $\rho_e = 1 - w_1$, and vary w_1 (0.5, 0.4, 0.3, 0.2, and 0.1). Note how the strong correlations create a dip in both the interacting DOS and the relaxation time near the fermi level. As w_1 is made smaller, the scattering time becomes more asymmetric in frequency, which should yield larger thermopowers. Note that there is residual scattering at the fermi energy as $\omega \rightarrow 0$, which should produce a finite value for the DC conductivity at $T = 0$ (recall the Falicov-Kimball model is not a fermi liquid in this regime).

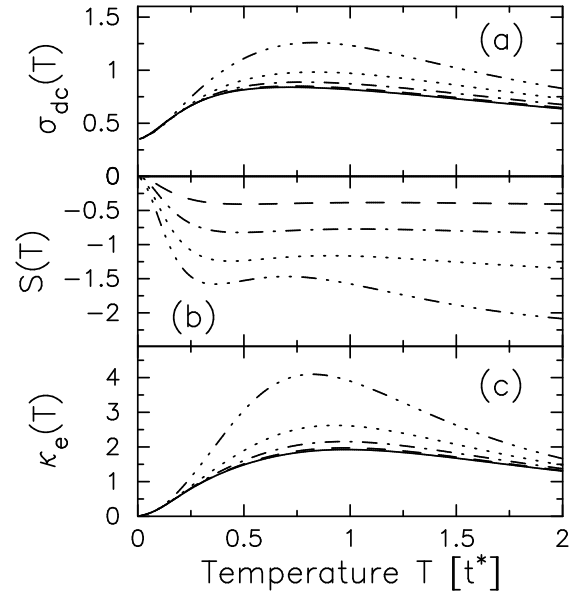


FIG. 2. (a) DC conductivity (in units of σ_0), (b) thermopower (in units of $k_B/|e|$), and (c) electronic contribution to the thermal conductivity (in units of $k_B^2\sigma_0/e^2$) for the Falicov-Kimball model at $U = 1$, $\rho_e = 1 - w_1$, and $w_1 = 0.5$ (solid), 0.4 (dashed), 0.3 (chain-dotted), 0.2 (dotted), and 0.1 (chain-triple-dotted).

We plot the DC conductivity, thermopower, and electronic contribution to the thermal conductivity in Fig. 2. The DC conductivity is fairly flat as a function of T over a wide temperature range, and is enhanced, as w_1 is made smaller (and the particle-hole asymmetry is enhanced). The thermopower is essentially flat at high temperature, increases as w_1 decreases, and then has a crossover to linear behavior below $T \approx 0.25t^*$. The slope of the low-temperature linear behavior increases as particle-hole asymmetry increases. The thermal conductivity is also essentially flat at high temperature, but then has a characteristic linear behavior that sets in below $T \approx 0.6t^*$. This behavior is typical of a metal that has significant scattering. Note that at low temperature, we might expect the Wiedemann-Franz law to hold, while at high temperature, the Lorenz number must decrease with T (since the ratio of the conductivities approaches a constant). The high temperature decrease of \mathcal{L} with a constant (or increasing) thermopower can lead to a large

thermoelectric figure of merit.

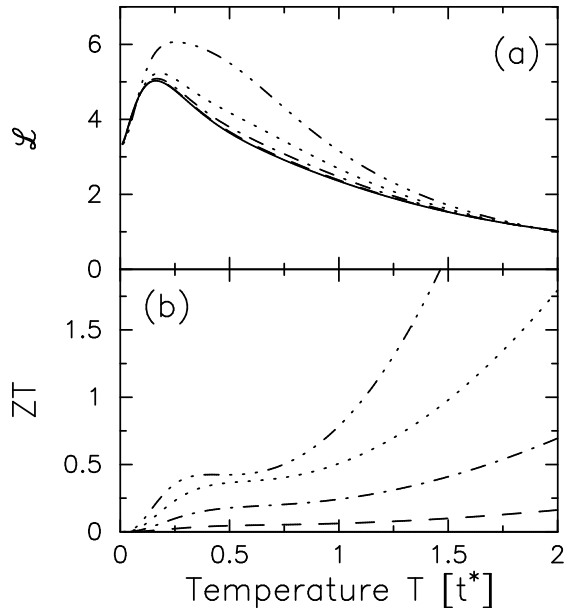


FIG. 3. (a) Lorenz number and (b) thermoelectric figure of merit for the Falicov-Kimball model at $U = 1$, $\rho_e = 1 - w_1$, and $w_1 = 0.5$ (solid), 0.4 (dashed), 0.3 (chain-dotted), 0.2 (dotted), and 0.1 (chain-triple-dotted).

The Lorenz number and thermoelectric figure of merit are plotted in Fig. 3. Note how the Lorenz number approaches $\pi^2/3$ as $T \rightarrow 0$. This follows whenever $\tau(\omega) \neq 0$ at $\omega = 0$, or whenever the interacting DOS at the chemical potential is nonzero. The decrease in \mathcal{L} at high T occurs because both the DC conductivity and the electronic contribution to the thermal conductivity become flat at high T . What is interesting is the moderate temperature peak in \mathcal{L} with the linear decrease toward the fermi-liquid value as $T \rightarrow 0$. This occurs because the system has strong scattering, which produces deviations from the Wiedemann-Franz law at moderate T . What is unfortunate is that an enhancement of \mathcal{L} leads to a reduction in ZT . This can be seen clearly in panel (b). The high-temperature figure of merit is large, and increases in magnitude as w_1 decreases due to the enhancement of the thermopower (since \mathcal{L} is independent of w_1 at high T). But the figure of merit rapidly decreases at low- T and indicates that strongly scattering metals of this type can not be used for thermoelectric applications at low temperature (but they would work fine at high T if κ_L was small enough, which is usually true).

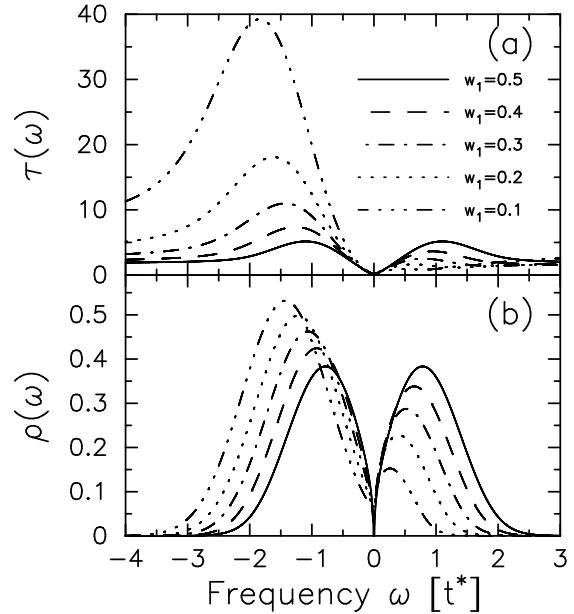


FIG. 4. (a) Effective scattering time and (b) interacting DOS for the Falicov-Kimball model at $U = 1.5$, $\rho_e = 1 - w_1$, and $w_1 = 0.5$ (solid), 0.4 (dashed), 0.3 (chain-dotted), 0.2 (dotted), and 0.1 (chain-triple-dotted). Now $\tau(\omega)$ has a quartic dependence on frequency, and the DOS becomes exponentially small in the “gap region”. The gap fills in for $w_1 < 0.25$ (which is difficult to see in the figure), so we expect the transport behavior to be different for small w_1 .

Next we show the evolution of the relaxation time and the interacting DOS as we move into the correlated insulator regime $U = 1.5$. Here the self energy develops a pole at $\omega = 0$ for $w_1 > 0.25$, which produces a narrow region of exponentially small DOS inside a “gap region”, but the pole disappears for small enough w_1 , and the system has strong scattering, but is still metallic as $T \rightarrow 0$. This is difficult to see in the above figure because we are not plotting the gap region on a logarithmic scale. We expect that the transport properties may differ depending on the value of w_1 for $U = 1.5$, but it should not be too dramatic because the metallic phase has very strong scattering.

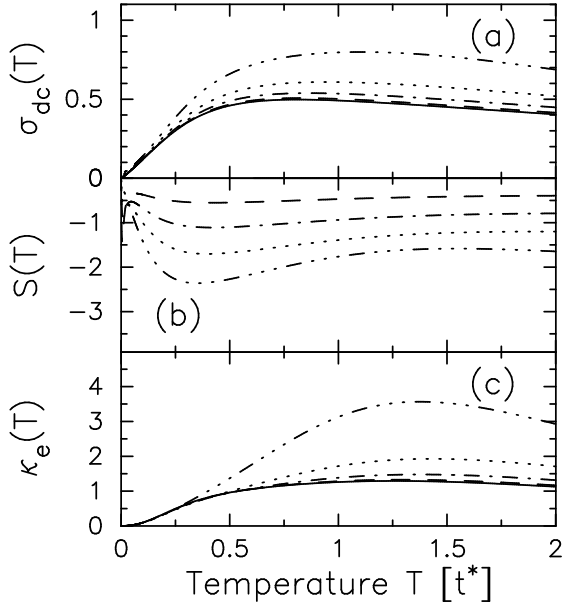


FIG. 5. (a) DC conductivity, (b) thermopower, and (c) electronic contribution to the thermal conductivity for the Falicov-Kimball model at $U = 1.5$, $\rho_e = 1 - w_1$, and $w_1 = 0.5$ (solid), 0.4 (dashed), 0.3 (chain-dotted), 0.2 (dotted), and 0.1 (chain-triple-dotted). Note the very low-temperature peak in the thermopower for $w_1 = 0.4$ and $w_1 = 0.3$.

The transport coefficients are plotted in Fig. 5. These look similar to those in Fig. 2 except now the conductivity vanishes as $T \rightarrow 0$ for the insulating phases and the thermal conductivity approaches zero faster than linearly for the insulators as well. In addition, when w_1 is close to half filling, we find a low- T peak in the thermopower. Our calculations indicate that the thermopower goes to zero as $T \rightarrow 0$, but we cannot rule out the possibility of a small nonzero value at $T = 0$ (the chemical potential, as a function of T , develops a large negative slope as $T \rightarrow 0$, but we cannot tell if the slope diverges).

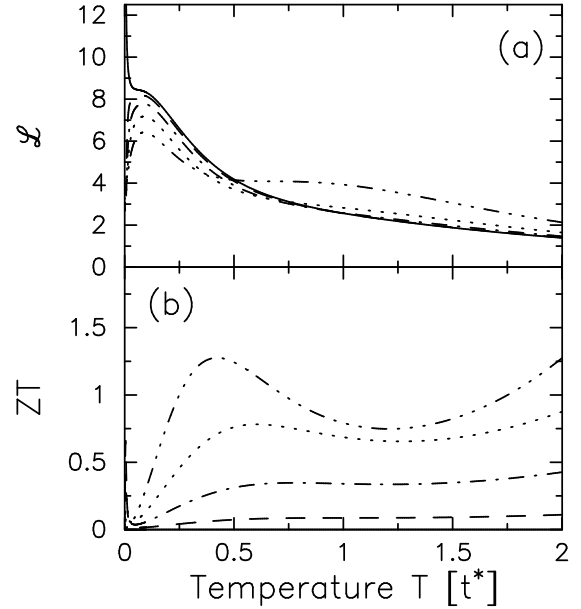


FIG. 6. (a) Lorenz number and (b) thermoelectric figure of merit for the Falicov-Kimball model at $U = 1.5$, $\rho_e = 1 - w_1$, and $w_1 = 0.5$ (solid), 0.4 (dashed), 0.3 (chain-dotted), 0.2 (dotted), and 0.1 (chain-triple-dotted).

The plot of the Lorenz number and of the thermoelectric figure of merit in Fig. 6 show a number of interesting features. First off, note the very large increase in \mathcal{L} as $T \rightarrow 0$ for the half-filled case versus all other fillings. This behavior happens because the half-filled case is qualitatively different from all other cases at low temperature. At half filling, the chemical potential is always at $U/2$ and has no temperature dependence. Hence the system always has a pseudogap-like behavior of the DOS, with it vanishing only at the fermi level. For all other cases, the chemical potential depends on T . Hence, at finite- T , the DOS at the chemical potential is nonzero, and only vanishes exactly at $T = 0$. This makes the low-temperature behavior away from half filling appear like that of a metal, resulting in the Wiedemann-Franz prediction for \mathcal{L} . Hence there is a low- T downturn to \mathcal{L} off of half filling. Second, at high temperature, \mathcal{L} has doping dependence now, which is a result of the fact that for $w_1 < 0.25$ the system is metallic, while for $w_1 > 0.25$ it is insulating. Third, the values of the thermoelectric figure of merit are enhanced at moderate temperature for low w_1 , and there is a low-temperature peak in ZT for $w_1 = 0.3$ and 0.4, which is hard to see in the figure (it is blown up in Fig. 10). Finally, the high-temperature behavior of ZT is actually reduced over that of the correlated metal because \mathcal{L} is somewhat larger and S is somewhat smaller here. ZT is also a flatter function of T here.

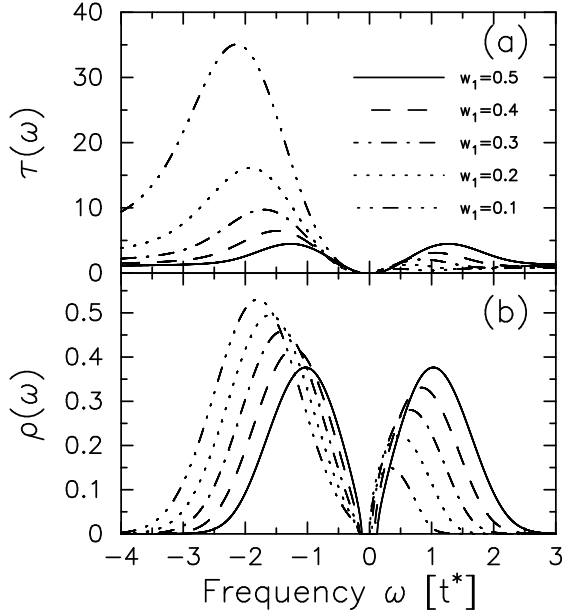


FIG. 7. (a) Effective scattering time and (b) interacting DOS for the Falicov-Kimball model at $U = 2$, $\rho_e = 1 - w_1$, and $w_1 = 0.5$ (solid), 0.4 (dashed), 0.3 (chain-dotted), 0.2 (dotted), and 0.1 (chain-triple-dotted).

We plot the relaxation time and interacting DOS for the case $U = 2$ in Fig. 7. Now all dopings have well-defined “gap regions”, but the size of the “gap” is still relatively small. Note that the effective relaxation time is quartic for all fillings here.

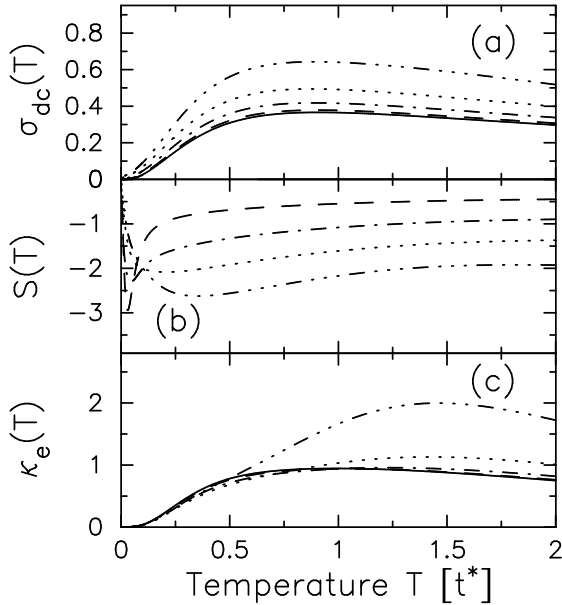


FIG. 8. (a) DC conductivity, (b) thermopower, and (c) electronic contribution to the thermal conductivity for the Falicov-Kimball model at $U = 2$, $\rho_e = 1 - w_1$, and $w_1 = 0.5$ (solid), 0.4 (dashed), 0.3 (chain-dotted), 0.2 (dotted), and 0.1 (chain-triple-dotted).

The transport coefficients are plotted in Fig. 8 for $U = 2$. Both the electrical and thermal conductivities behave as expected, with exponentially small values at low T (but the “gap” decreases as w_1 decreases, so the exponent is doping dependent). The thermopower still has an interesting low-temperature peak. The peak height moves out to larger T and broadens as U is increased and as w_1 is decreased. We expect this will have a significant impact on ZT .

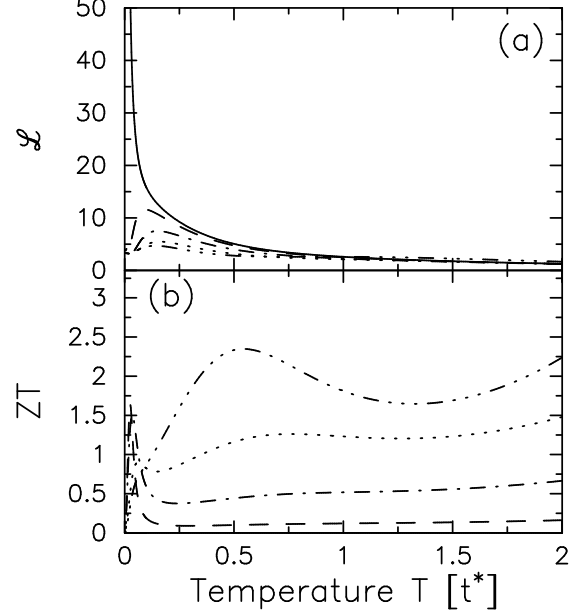


FIG. 9. (a) Lorenz number and (b) thermoelectric figure of merit for the Falicov-Kimball model at $U = 2$, $\rho_e = 1 - w_1$, and $w_1 = 0.5$ (solid), 0.4 (dashed), 0.3 (chain-dotted), 0.2 (dotted), and 0.1 (chain-triple-dotted).

The Lorenz number becomes huge (but does not appear to diverge) in the correlated insulator at half filling, but continues to have the low- T peak and return to $\pi^2/3$ as $T \rightarrow 0$ away from half filling. The thermoelectric figure of merit has a sharp peak at low temperature, whose width and peak location increase with an increase of U and a decrease of w_1 . Note that the low- T peak is associated with the sharp drop in \mathcal{L} at low temperature, which seems to occur only when one has pseudogap behavior and a chemical potential that moves away from the point where the DOS vanishes at finite T . Nevertheless, the peak is rather striking and does show that $ZT > 1$ is possible in an all electronic system. Since the electronic contribution to the thermal conductivity exponentially decreases at low temperature, while the lattice contribution decreases as a cubic power law (when one is well below the Debye energy), we expect that at very low temperatures the thermal conductivity will be dominated by a lattice contribution, and if that contribution is significantly larger than the electronic contribution, then the low- T peak in ZT will go away.

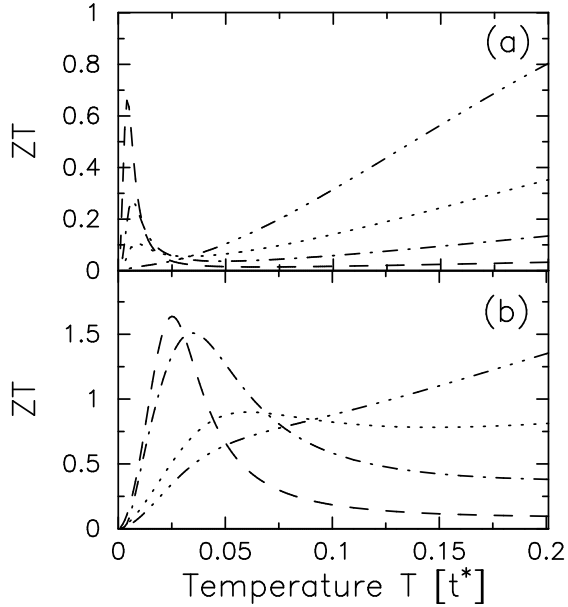


FIG. 10. Blow-up of the low-temperature region for the thermoelectric figure of merit with (a) $U = 1.5$ and (b) $U = 2$. The curves correspond to $w_1 = 0.5$ (solid), 0.4 (dashed), 0.3 (chain-dotted), 0.2 (dotted), and 0.1 (chain-triple-dotted). Note how the peak can be pushed to very low T and to reasonably high values when U is tuned to lie close to the critical U of the metal-insulator transition. The peak generically moves to higher T , increases in magnitude, and broadens as U is increased.

We blow up the ZT plots for the low temperature region in Fig. 10. Note how one can find a sharp peak with an enhanced ZT at low temperature when one is close to the metal-insulator transition. As U is increased, the magnitude of the peak increases and broadens, but it is pushed to higher values of temperature. We expect that the lattice contribution to the thermal conductivity may significantly reduce this peak, or may even destroy it, but in both cases, the thermal conductivity at the low- T peak is about 10^{-4} the value at high T and perhaps the lattice thermal conductivity could be low enough that it would not significantly interfere with the peak.

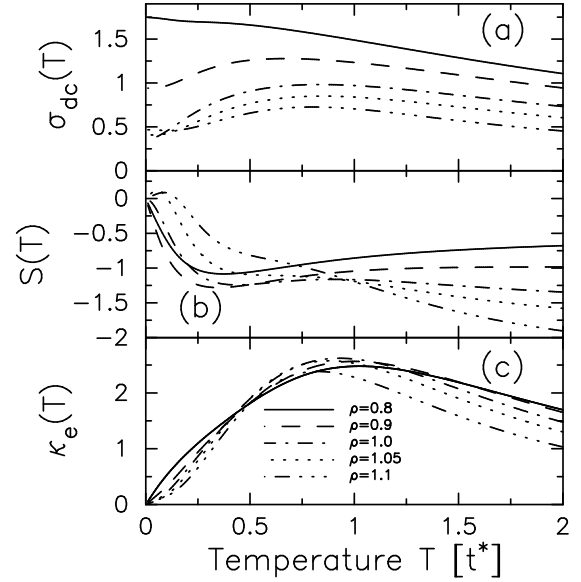


FIG. 11. (a) DC conductivity, (b) thermopower, and (c) electronic contribution to the thermal conductivity for the Falicov-Kimball model at $U = 1$, $w_1 = 0.2$, and $\rho_e + w_1 = 0.8$ (solid), 0.9 (dashed), 1.0 (chain-dotted), 1.05 (dotted), and 1.1 (chain-triple-dotted).

We conclude our presentation of results by showing what happens when the system is forced to be metallic, by pushing the electronic chemical potential away from the “gap region”. We start with the strongly correlated metal at $U = 1$ and $w_1 = 0.2$, but we vary the total concentration to be 0.8 (solid), 0.9 (dashed), 1.0 (chain-dotted), 1.05 (dotted), and 1.1 (chain-triple-dotted). The relaxation time and the interacting density of states can be read off of the $w_1 = 0.2$ curves in Fig. 1, with the only change an overall shift of the origin for the different electronic fillings. The transport coefficients are plotted in Fig. 11. As expected, the system is least conductive when the filling is equal to 1 (corresponding to the chemical potential at the “kink” in the interacting DOS). The thermopower is enhanced at low temperature as we approach a total filling of one from below and suppressed at high temperature. The converse occurs for fillings larger than 1—the low-temperature thermopower is reduced and the high-temperature is enhanced. This suggests that the thermoelectric properties at high temperature may be enhanced by increasing the electron filling.

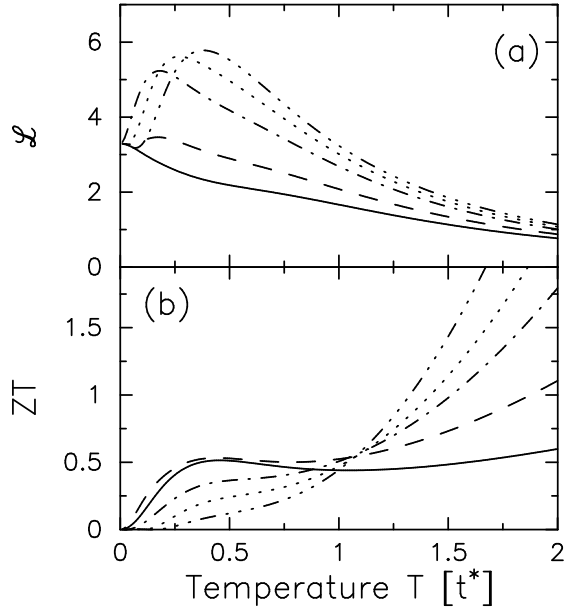


FIG. 12. (a) Lorenz number and (b) thermoelectric figure of merit for the Falicov-Kimball model at $U = 1$, $w_1 = 0.2$, and $\rho_e + w_1 = 0.8$ (solid), 0.9 (dashed), 1.0 (chain-dotted), 1.05 (dotted), and 1.1 (chain-triple-dotted).

The Lorenz number and thermoelectric figure of merit are plotted in Fig. 12. Note how the peak in the Lorenz number only occurs for total fillings larger than about 0.85, and how it gets larger and moves to higher temperature as the electronic filling increases. This has an obvious effect on ZT : we find ZT is enhanced at low temperature for fillings less than 1, and is enhanced at high temperature for fillings greater than 1. These effects can be significant.

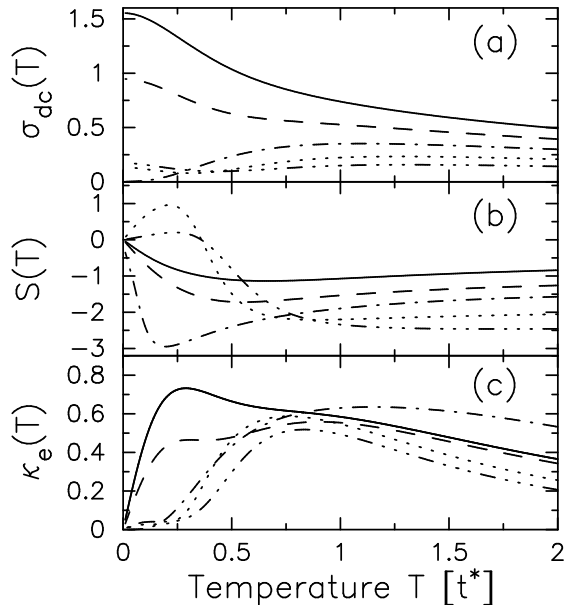


FIG. 13. (a) DC conductivity, (b) thermopower, and (c) electronic contribution to the thermal conductivity for the Falicov-Kimball model at $U = 3$, $w_1 = 0.2$, and $\rho_e + w_1 = 0.8$ (solid), 0.9 (dashed), 1.0 (chain-dotted), 1.05 (dotted), and 1.1 (chain-triple-dotted).

Finally, we examine a strongly correlated insulator with $U = 3$ and $w_1 = 0.2$. We don't plot the relaxation time and DOS here, because it is similar to what is seen for $U = 2$, but with a somewhat larger “gap region”. The transport coefficients are plotted in Fig. 13. Here we see a marked difference between the metallic cases, with total filling not equal to 1 and the insulating case where it equals 1. In particular, the DC conductivity rises as T decreases, as expected for a metal, but it is exponentially suppressed in the insulator. The thermal conductivity is similar, with well-developed linear regimes for the metallic systems (that are better defined for fillings less than 1), and “gapped” behavior for the insulator. The thermopower has quite interesting behavior. For fillings less than 1, we see a dramatic enhancement in the low-temperature thermopower as we approach the insulator. For fillings above 1, we see the thermopower has a sign change. This sign change is easy to understand. When the total filling lies in the range between 1 and 1.1, the electronic chemical potential lies in the lower half of the upper Hubbard band at low temperature. Hence at low- T , the thermopower should appear to be electron-like (positive). But as T is increased, the influence of the gap becomes smaller, and the system looks overall hole-like because the chemical potential is in the top part of the overall “bandstructure”. The crossover temperature should be on the order of the size of the “gap region”. In addition to this sign change, we see a large enhancement of the high-temperature thermopower as the filling increases. This is also expected because the chemical potential is moving higher and higher in the band.

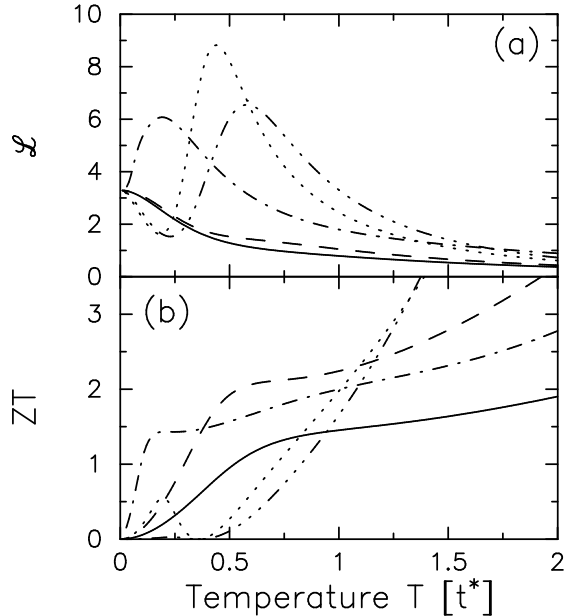


FIG. 14. (a) Lorenz number and (b) thermoelectric figure of merit for the Falicov-Kimball model at $U = 3$, $w_1 = 0.2$, and $\rho_e + w_1 = 0.8$ (solid), 0.9 (dashed), 1.0 (chain-dotted), 1.05 (dotted), and 1.1 (chain-triple-dotted).

We end with the Lorenz number and thermoelectric figure of merit for $U = 3$ and $w_1 = 0.2$ in Fig. 14. The behavior here is also quite interesting. The Lorenz number is monotonic for total filling less than one, but then shows a large peak at a filling of 1. When the filling increases further, it develops a lower-temperature dip below a higher-temperature peak. This low-temperature dip can be advantageous to thermoelectric properties, but unfortunately the thermopower is too low (since it passes through zero) in this region to create a large ZT . Nevertheless, we do see interesting phenomena in the ZT curves as well. As we approach a total filling of 1, the low-temperature shoulder gets pushed closer to $T = 0$, and it remains at a fairly high value, above 1. When we move past 1, we find the low- T figure of merit is small due to the proximity to the sign change in S , but the high-temperature values are strongly enhanced.

IV. CONCLUSIONS

We have examined the thermal transport properties of the Falicov-Kimball model in a binary-alloy picture. By fixing the ion concentration as a function of temperature, we force the renormalized energy level of the localized particles to lie at the chemical potential as $T \rightarrow 0$, which is believed to be advantageous for thermal transport. Indeed, we find significant regions of parameter space with $ZT > 1$ at high temperature, and in the correlated insulators, we also find a small region of parameter space with $ZT > 1$ at low temperature. Our calculations neglect the lattice contribution to the thermal conductivity,

which should have a limited effect on the high temperature calculations, but can destroy the low-temperature peaks in ZT if the lattice thermal conductivity is too big.

We showed that generically, in a correlated insulator, one has $S \rightarrow 0$ as $T \rightarrow 0$ and $\mathcal{L} \rightarrow \infty$ as $T \rightarrow 0$. Our analysis for the thermopower emphasized a relationship between S and the temperature dependence of the chemical potential, which appears to be general for systems that display a true gap. The generic dependences of S and \mathcal{L} at low temperature imply that the generic thermoelectric figure of merit would be small at low temperature. But in the infinite-dimensional hypercubic lattice, the noninteracting DOS is a Gaussian, which implies that the system really possesses a pseudogap in the correlated insulator, with the interacting DOS exponentially small in the gap region. This has a significant effect on the thermal transport because the relaxation time is not exponentially small within the “gap region”, and in particular, it can produce a low-temperature peak to ZT that moves to lower temperature as w_1 approaches 0.5 and as U is tuned to lie close to the metal-insulator transition. If we took the hopping energy scale t^* to be on the order of 1 eV, then the low-temperature peak in ZT can easily occur below 50 K [see Fig. 10 where the peak in panel (a) lies at about $T = 0.003$]. The key issue is whether or not the lattice thermal conductivity would wash out this effect.

One question to ask, then, is can one find a way to introduce an exponentially small DOS into the gap region of a correlated insulator (if they do not appear in the bulk system)? The answer is yes, and it can be done by creating heterostructures of the correlated material and metals. The metallic DOS will “leak” into the correlated insulator, with a characteristic length scale, and create small subgap DOS within the system. Hence we believe the heterostructure idea of Mao and Bedell⁷ or Rontani and Sham⁶ can indeed allow one to get large peaks in the low-temperature figure of merit (if the exponentially small DOS also leads to a much larger “effective” scattering time). Since a heterostructure will also reduce the lattice thermal conductivity, it is possible that the low-temperature peak could be realized, but it is likely to require a careful tuning of the correlation gap, and the thicknesses of the metallic and correlated layers of the heterostructure. One also has to be able to maintain the correlated behavior within the thin layers of the heterostructure.

Another potential way to create states within the gap is simply via a thermal rearrangement of the DOS within the bulk system as T increases. In the Falicov-Kimball model, the interacting DOS is T -independent, but in other correlated systems (like the Hubbard or periodic Anderson models) the correlated DOS does depend on T . It would be interesting to see if the creation of an exponentially small DOS via thermal activation could allow for a peak in the low-temperature thermoelectric figure of merit (but this cannot be studied with the Falicov-Kimball model).

The situation at high temperature is much more promising. We find that generically both the electrical and thermal conductivities become flat at high temperature, so the Lorenz number decreases like $1/T$. The thermopower also becomes flat, with a magnitude growing as the system is made more particle-hole asymmetric. The net effect is a thermoelectric figure of merit that grows linearly in T , with a potentially large slope. We found the figure of merit usually improved at high temperature when the electronic filling was pushed higher in the band, and that there was no magical need to tune the electronic chemical potential to lie in the “gap region”, rather the enhancement was generic in correlated systems.

We finally note that our scattering time $\tau(\omega)$ is never close in appearance to a delta function in this system. It can develop large asymmetry with a large peak lying at one side of the chemical potential, but the peak width is always broad, and determined by the effective bandwidth of the conduction electrons. This is, of course, because we have no hybridization in this model, which precludes the appearance of a sharp Abrikosov-Suhl resonance in the DOS and the similar formation of such a structure in $\tau(\omega)$. It would be interesting to see how the situation could change if hybridization was included, but this requires significantly more sophisticated numerical efforts.

ACKNOWLEDGMENTS

This work was supported by the National Science Foundation under grants DMR-9973225 and DMR-0210717. J.K.F. thanks the hospitality of the Kavli Institute of Theoretical Physics, where the majority of this work was completed. At the KITP, the research was supported in part by the National Science Foundation under Grant No. PHY99-07949. V.Z. thanks the Swiss National Science Foundation grant no. 7KRPJ65554.

- J. M. Rowell, N. Newman, and A. J. Freeman, Phys. Rev. B **65**, 245110 (2002).
- ¹¹ W. Metzner and D. Vollhardt, Phys. Rev. Lett. **62**, 324 (1989).
- ¹² U. Brandt and C. Mielsch, Z. Phys. B **75**, 365 (1989); **79**, 295 (1990); U. Brandt, A. Fledderjohann, and G. Hülsenbeck, *ibid.* **81**, 409 (1990); U. Brandt and C. Mielsch, *ibid.* **82**, 37 (1991).
- ¹³ J.K. Freericks and V. Zlatić, Phys. Rev. B **58**, 322 (1998).
- ¹⁴ V. Zlatić, J.K. Freericks, R. Lemański, and G. Czycholl, Phil. Mag. B **81**, 1443 (2001).
- ¹⁵ P. G. J. van Dongen and C. Leinung, Ann. Phys. (Leipzig) **6**, 45 (1997).
- ¹⁶ R. Kubo, J. Phys. Soc. Japan **12**, 570 (1957); D.A. Greenwood, Proc. Phys. Soc. (London) **71**, 585 (1958).
- ¹⁷ A. Khurana, Phys. Rev. Lett., **64**, 1990 (1990).
- ¹⁸ G.D. Mahan, *Many-Particle Physics*, (New York, Plenum, 1990).
- ¹⁹ M. Jonson and G.D. Mahan, Phys. Rev. B **21**, 4223 (1980); *ibid.* **42**, 9350 (1990).
- ²⁰ N. W. Ashcroft and N. D. Mermin, *Solid State Physics*, (Philadelphia, Holt, Rinehart and Winston, 1976).
- ²¹ G.V. Chester and A. Thellung, Proc. Phys. Soc. (London) **77**, 1005 (1961); N.F. Mott and E.A. Davis, *Electronic Processes in Non-Crystalline Materials*, (Clarendon, Oxford, 1971) p. 47.
- ²² J. K. Freericks and V. Zlatić, Phys. Rev. B **64**, 073109 (2001).
- ²³ C. Villagonzalo and R. Römer, Ann. Phys. (Leipzig) **7**, 394 (1998); C. Villagonzalo, R. Römer, and M. Schreiber, Eur. Phys. J. (France) B **12**, 179 (1999); Ann. Phys. (Leipzig) **8**, Spec. Issue SI-269 (1999); C. Villagonzalo, R. Römer, M. Schreiber, and A. MacKinnon, Phys. Rev. B **62**, 16446 (2000).
- ²⁴ J. Hubbard, Proc. Roy. Soc. (London) **A276**, 238 (1963).
- ²⁵ V. S. Oudovenko and G. Kotliar, Phys. Rev. B **65**, 075102 (2002).

¹ G. Mahan, B. Sales, and J. Sharp, Phys. Today, 42 (March, 1997).

² J. C. Peltier, Ann. de Chimie, **LVI**, 371 (1834).

³ T. J. Seebeck, Abhandlung der Deutschen Akademie der Wissenschaften zu Berlin, 265 (1822).

⁴ D. M. Rowe and C. M. Bhandari, *Modern Thermoelectrics* (London: Holt, Rinehart, and Winston, 1983), Ch. 2.

⁵ G.D. Mahan, Solid State Phys. **51**, 81 (1998).

⁶ M. Rontani and L. J. Sham, J. Appl. Phys. **77**, 3033 (2000).

⁷ W. Mao and K. S. Bedell, Phys. Rev. B **59**, R15590 (1999).

⁸ G. D. Mahan and J. O. Sofo, Proc. Natl. Acad. Sci. (USA) **93**, 7436 (1996).

⁹ L.M. Falicov and J.C. Kimball, Phys. Rev. Lett. **22**, 997 (1969)

¹⁰ L. Yu, C. Stampfl, D. Marshall, T. Eshrich, V. Narayanan,